

Defect band-gap structures for triggering single-photon emission

Ho Trung Dung*, Ludwig Knöll, and Dirk-Gunnar Welsch

Theoretisch-Physikalisches Institut, Friedrich-Schiller-Universität Jena, Max-Wien-Platz 1, 07743 Jena, Germany

(Oct. 14, 2002)

A 3D analysis of the spontaneous decay of a single dipole embedded in a planar multilayer structure is given, with special emphasis on Kerr-tunable photonic band-gap materials for single-photon emission on demand. It is shown that the change in the density of states near a defect resonance is much more pronounced than that one near the band edges. In particular, operation near the band edge as suggested from a 1D analysis is little suited for controlling the photon emission.

PACS numbers: 42.70.Qs, 42.50.Dv, 03.67.Dd

Quantum states of light hold promise for applications in transmission, storage, and processing of information in new and powerful ways. Among them, the single-photon states are of particular interest. They are crucial in enabling secure transmission of information without risk of eavesdropping [1], and could be useful in all-optical quantum information processing devices [2]. One of the most natural ways to generate single-photon states is through controlled radiation of a single emitter, which, after delivering a photon, is necessarily in the ground state and will not produce another one before being reexcited. Various schemes have been reported, such as single-atom passage through high- Q cavities in the strong-coupling regime [3–6], regulated injection of electron-hole pairs into mesoscopic quantum wells [7], and fluorescence light from individual nitrogen-vacancy color centers in diamond [8–10], from molecules [11–16], and from semiconductor quantum dots [17–23].

In practice, single-photon sources that operate in a single-mode regime and ensure a sufficiently high collection efficiency of the emitted photon are desired to be used. A promising route to achieve these goals is to place the dipole emitters within distributed Bragg reflector Fabry-Perot [11,12] or pillar [20,22,23] microcavities. Due to a strong Purcell selective enhancement of spontaneous emission, photons are predominantly emitted into the cavity mode, with a high directionality in the far-field zone. To truly produce photons one by one, the excitation duration is commonly required to be short compared to the emitter lifetime. Note that more than one photon triggered in one shot can, e.g., render quantum cryptography insecure under certain types of eavesdropping attacks [1].

Recently, a novel ‘photon-gun’ scheme for generating single photons on demand has been suggested which is based on the possibility of controlling spontaneous emission in a photonic band-gap material [24]. An initially excited dipole is embedded within a band-gap structure

made of Kerr-nonlinear material such that the transition frequency of the dipole is inside the band gap, in fact near its edge, where the spontaneous decay is strongly inhibited. By applying an external pump field, thanks to Kerr nonlinearity, the refractive index of the structure is changed and, as a consequence, the band gap is shifted in such a way that the dipole transition frequency falls just outside the gap, into a region of high density of states. The dipole is then forced to decay rapidly by emitting a photon. In particular, the scheme offers the advantage of temporally separating the excitation and the emission process, thereby putting less constraint on the duration of the excitation.

However, the underlying theory in [24] is strictly one-dimensional, thus completely disregarding the dipole emission into oblique directions. As we shall show below, this leads to a drastic over-estimation of the density-of-state switch at the band edge which can be realized by employing the Kerr effect. Three-dimensional description of the spontaneous decay of an excited dipole in planar band-gap structures has been given in [25–27], with special emphasis on the limiting case of an infinitely large number of slabs [25], the interference between two decay channels [26], and the dependence of the decay rate on the position of the dipole [27]. In all these studies as well as in [24] material dispersion and absorption are ignored.

From a 3D theory, we show that there is little chance of realizing the photon-gun as proposed in [24]. We therefore introduce a defect into the band-gap structure – a periodic double-layer of quarter-wave plates – by increasing the thickness of the layer containing the emitter dipole from a quarter to a half wavelength. The structure is now essentially a Fabry-Perot microcavity whose boundaries are formed by distributed Bragg reflectors, with the defect resonance inside the band gap being the fundamental resonance of the cavity. Comparing the operation of the device near the band edge and near the defect resonance, we show that only in the latter case a controlled photon emission may be realized. Finally, we briefly discuss the effect of material absorption and give an outlook for further improvements.

The system under study consists of a dipole emitter, which can be an atom, ion, molecule, semiconductor quantum dot, or nanocrystal, placed in a photonic band-gap structure consisting of quarter-wave plates of infinite lateral extension and periodically interchanging low and high complex permittivities $\epsilon_L(\omega)$ and $\epsilon_H(\omega)$ (Fig. 1). The dipole excitation can be realized by using stimulated Raman adiabatic passage [28] with the frequencies of both branches of the Raman transition ly-

ing outside the band gap, or, in the case of a molecular emitter, by using nonresonant optical pumping of a vibronic state within the manifold of vibrational states in the upper electronic state followed by a fast relaxation to the emission-ready state.

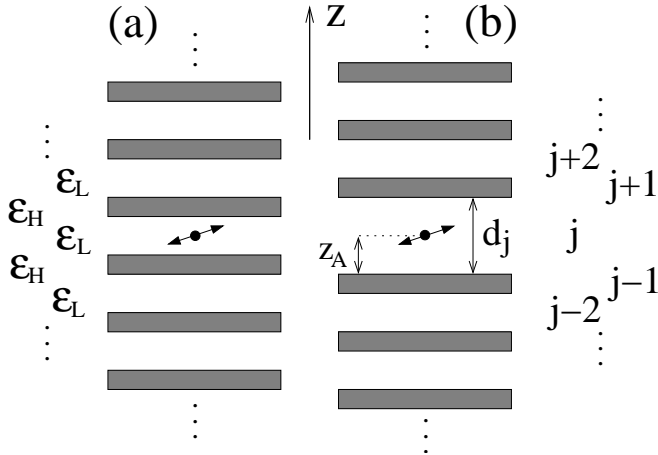


FIG. 1. A dipole embedded in a band-gap structure (a) with no defect and (b) with a defect in the form of a half-wavelength thick layer.

The spontaneous decay rate of a dipole (position \mathbf{r}_A , transition frequency ω_A , transition dipole moment \mathbf{d}_A) that is surrounded by arbitrary, dispersing and absorbing bodies can be determined according to the formula [29,30]

$$\Gamma = \frac{2\omega_A^2}{\hbar\epsilon_0 c^2} \mathbf{d}_A \text{Im} \mathbf{G}(\mathbf{r}_A, \mathbf{r}_A, \omega_A) \mathbf{d}_A, \quad (1)$$

where $\mathbf{G}(\mathbf{r}, \mathbf{r}', \omega)$ is the (classical) Green tensor of the medium-assisted Maxwell-field. Note that ω_A already includes the medium-induced level shift. The (equal-position) Green tensor can be decomposed into two parts,

$$\mathbf{G}(\mathbf{r}_A, \mathbf{r}_A, \omega) = \mathbf{G}^{\text{bulk}}(\mathbf{r}_A, \mathbf{r}_A, \omega) + \mathbf{G}^{\text{refl}}(\mathbf{r}_A, \mathbf{r}_A, \omega), \quad (2)$$

where $\mathbf{G}^{\text{bulk}}(\mathbf{r}_A, \mathbf{r}_A, \omega)$ is the Green tensor for bulk material and $\mathbf{G}^{\text{refl}}(\mathbf{r}_A, \mathbf{r}_A, \omega)$ is the reflection part that insures the correct boundary conditions at the surfaces of discontinuity.

Let z be the direction of variation of the permittivity of the multilayer system and the dipole be located in the j th layer (Fig. 1). Within the frame of the real-cavity model of the local-field correction, the part of the dipole decay rate caused by the bulk Green tensor reads as [30]

$$\begin{aligned} \Gamma^{\text{bulk}} = \Gamma_0 & \left| \frac{3\epsilon_j}{2\epsilon_j + 1} \right|^2 \left\{ n'_j \right. \\ & + \frac{\epsilon''_j}{|\epsilon_j|^2} \left[\left(\frac{c}{\omega_A R} \right)^3 + \frac{28|\epsilon_j|^2 + 16\epsilon'_j + 1}{5|2\epsilon_j + 1|^2} \left(\frac{c}{\omega_A R} \right) \right. \\ & \left. \left. - \frac{2}{|2\epsilon_j + 1|^2} (2n''_j |\epsilon_j|^2 + n''_j \epsilon'_j + n'_j \epsilon''_j) \right] \right\} \\ & + O(\omega_A R/c), \end{aligned} \quad (3)$$

where $\Gamma_0 = \omega_A^3 d_A^2 / (3\hbar\pi\epsilon_0 c^3)$ is the well-known decay rate in free space, $\epsilon_j = \epsilon_j(\omega_A) = \epsilon'_j + i\epsilon''_j$, $n_j = \sqrt{\epsilon_j} = n'_j + in''_j$, and R is the cavity radius that is assumed to be negligibly small compared with all characteristic lengths of the configuration under consideration. The reflection part of the Green tensor can be given in the form of [31]

$$\begin{aligned} \mathbf{G}^{\text{refl}}(\mathbf{r}_A, \mathbf{r}_A, \omega) \\ = \frac{i}{4\pi} \int_0^\infty dk_{\parallel} k_{\parallel} \frac{e^{i\beta_j d_j}}{2\beta_j} \tilde{\mathbf{G}}^{\text{refl}}(\mathbf{r}_A, \mathbf{r}_A, \omega, k_{\parallel}) \end{aligned} \quad (4)$$

[$k_j = \sqrt{\epsilon_j(\omega)} \omega/c$; $\beta_j = (k_j^2 - k_{\parallel}^2)^{1/2}$], where the nonvanishing components of $\tilde{\mathbf{G}}^{\text{refl}}$ are

$$\tilde{G}_{xx}^{\text{refl}} = \tilde{G}_{yy}^{\text{refl}} = -\frac{\beta_j^2}{k_j^2} C_-^p + C_+^s, \quad \tilde{G}_{zz}^{\text{refl}} = 2 \frac{k_{\parallel}^2}{k_j^2} C_+^p, \quad (5)$$

with

$$\begin{aligned} C_{+(-)}^q = \left[r_-^q e^{i\beta_j(2z_A - d_j)} + r_+^q e^{-i\beta_j(2z_A - d_j)} \right. \\ \left. + (-) 2r_+^q r_-^q e^{i\beta_j d_j} \right] D_q^{-1}, \end{aligned} \quad (6)$$

$$D_q = 1 - r_+^q r_-^q e^{2i\beta_j d_j}. \quad (7)$$

Here, $p(s)$ refers to TM(TE) polarized waves ($q=p, s$), and $r_{+(-)}^q$ are the total reflection coefficients at the upper (lower) stack of layers, which are to be calculated using recurrence formulas [31]. In the numerical calculation, material dispersion and absorption are taken into account through a permittivity of Drude-Lorentz type

$$\epsilon(\omega) = 1 + \frac{\omega_P^2}{\omega_T^2 - \omega^2 - i\omega\gamma}, \quad (8)$$

where ω_P corresponds to the coupling constant, and ω_T and γ are respectively the medium oscillation frequency and the linewidth. Note that for small absorption, the pole singularities in the Sommerfeld integrals appearing in Eq. (4) remain close to the $\text{Re}(k_{\parallel})$ axis and might cause serious problems. This can be avoided by deforming the integration path in the complex plane [32].

An example of the frequency response of the rate of spontaneous decay of a dipole in a band-gap structure according to Fig. 1(a) is shown in Fig. 2(a). It is seen that near the band edge the decay rate can be regarded as being a multiple-step function of frequency rather than a single-step function as in a 1D theory [24]. In particular, a change of the real part of the permittivity $\epsilon_H(\omega_0)$ from $\epsilon'_H(\omega_0) = 4$ to $\epsilon'_H(\omega_0) = 4.0804$ (ω_0 , mid-gap frequency) is seen to change the decay rate, for $\omega_A = 1.217 \omega_0$, from $\Gamma = 0.35 \Gamma_0$ to $\Gamma = 0.6 \Gamma_0$, which is far below the change from $\Gamma \simeq 0$ to $\Gamma = 50 \Gamma_0$, as it is predicted from the 1D theory in [24]. In this context it should be pointed out that in the 1D theory the change of the spontaneous decay near the band edge significantly increases with the number of layers, which is in strong contrast to the 3D theory where the available change effectively decreases.

To improve the performance of the device, we suggest to introduce a defect in the form of a half-wave plate and to operate it near the resulting defect resonance rather than near the band edge. The frequency response of the decay rate observed in that case is illustrated in Fig. 2(b). For the same change of the permittivity as in Fig. 2(a), the decay rate now changes from $\Gamma = 0.25\Gamma_0$ to $\Gamma = 2.26\Gamma_0$, that is a change of one order of magnitude becomes feasible. Moreover, the change is much more abrupt than in Fig. 2(a), which is of course an added bonus.

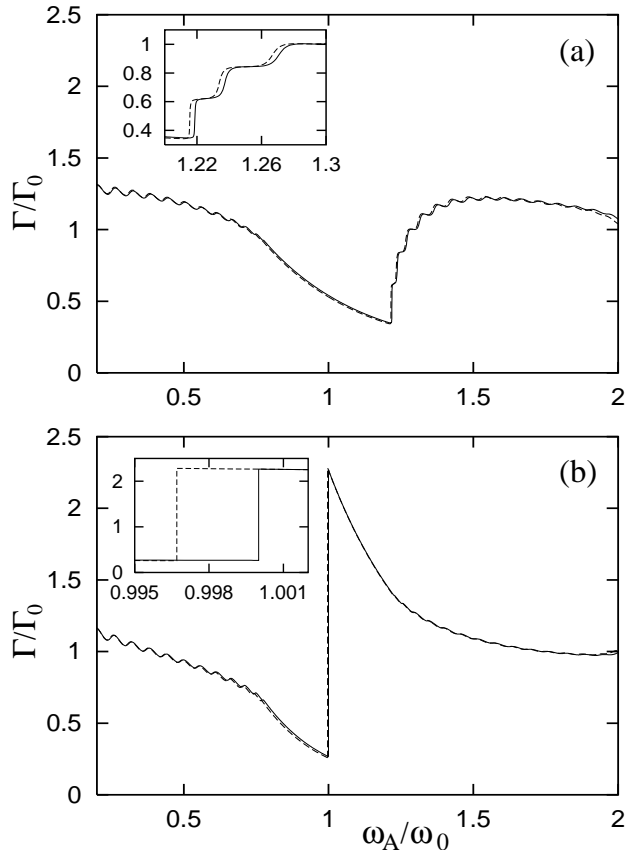


FIG. 2. (a) The decay rate of an x -oriented dipole located at the center of the middle layer of a 30-period structure is shown as a function of the transition frequency for $\varepsilon_j = \varepsilon_L = 1$ and $\varepsilon_H(\omega)$ from Eq. (8) with $\omega_T = 20\omega_0$, $\gamma = 10^{-7}\omega_0$, and $\omega_P = 1.7299\omega_T$ [$\varepsilon_H(\omega_0) \simeq 4 + i7.5 \times 10^{-10}$; solid line] and $\omega_P = 1.7529\omega_T$ [$\varepsilon_H(\omega_0) \simeq 4.0804 + i7.7 \times 10^{-10}$; dashed line]. (b) Normalized decay rate when a defect is introduced in the form of a half-wavelength thick middle layer. The other parameters are the same as in Fig. 2(a)

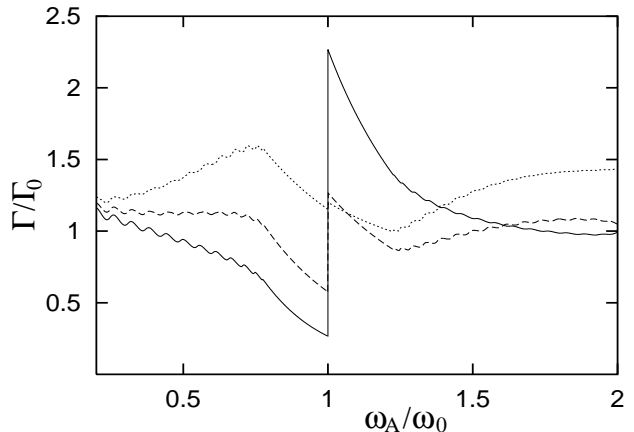


FIG. 3. The transition frequency dependence of the dipole decay rate in Fig. 2(b) is shown for different dipole positions: $z_A = 0.5d_j$ (solid line), $z_A = 0.2d_j$ (dashed line), and $z_A = 0.05d_j$ (dotted line). The permittivity $\varepsilon_H(\omega)$ is given according to Eq (8) with $\omega_T = 20\omega_0$, $\gamma = 10^{-7}\omega_0$, and $\omega_P = 1.7299\omega_T$. The other parameters are the same as in Fig. 2(b).

Figure 3 illustrates the influence of the position of the dipole on the frequency dependence of the decay rate for a defect-multilayer structure according to Fig. 1(b). It is seen that when the dipole is located in the middle of the layer, then the change of the decay rate at the defect resonance is most abrupt and thus best suited for the device operation.

So far we have assumed that the dipole orientation is parallel to the layers, e.g., in x -direction. In practice, this may not always be the case. In Fig. 4, we have plotted the frequency response of the decay rate for an x - and a z -oriented dipole and the decay rate averaged over all possible dipole orientations. Let us assume that $\varepsilon_j(\omega_A)$ can be regarded as being real. Decomposing the integral in Eq. (4) into two parts, $\int_0^{k_j} \dots + \int_{k_j}^\infty \dots$, we can distinguish between propagating and evanescent waves in the z -direction. Numerical computations (not shown) indicate that the abrupt change of the decay rate of an x -oriented dipole near the band edge [Fig. 4(a) for a structure according to Fig. 1(a)] and near the defect resonance [Fig. 4(b) for a structure according to Fig. 1(b)] is closely related to the case that the decay is associated with propagating-wave excitation, in which case the emitted photon can really escape the structure and subsequently be collected. On the contrary, a z -oriented dipole is stronger coupled to the evanescent field than to the propagating field, and thus does not feel the (quasi-)forbidden frequency range (see Fig. 4). Since this undesired effect is more pronounced for the perfect band-gap structure [Fig. 4(a)] than for the structure with the defect in [Fig. 4(b)], a single-photon source operating near a defect resonance is much more robust against a randomization of the dipole orientation than the one operating near the band edge of a defect-free structure.

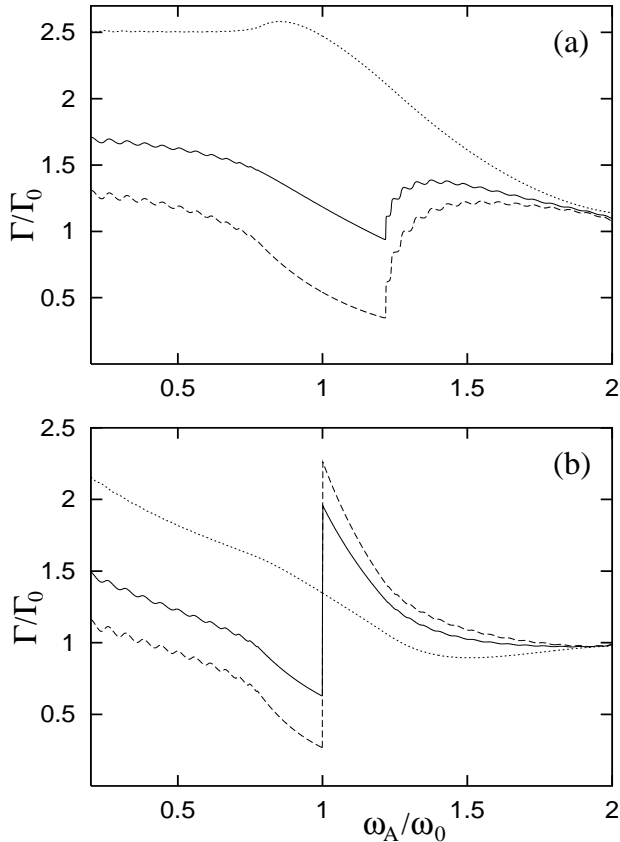


FIG. 4. Decay rate for an x -oriented dipole (dashed line), a z -oriented dipole (dotted line), and the averaged decay rate [$\Gamma = \frac{1}{3}(2\Gamma_x + \Gamma_z)$; solid line]. Case (a) refers to the band-gap structure without defect [Fig. 1(a)], while case (b) refers to the structure with the defect [Fig. 1(b)]. The dipole is located at the center of the middle layer. The other parameters are the same as in Fig. 3.

In Fig. 5 the effect of material absorption on the decay rate near the defect resonance is illustrated. As expected, absorption tends to smooth the change of the decay rate at the defect resonance. For $\gamma = 10^{-7}\omega_0$ and a relative change of $\varepsilon'_H(\omega_0)$ of the order of 10^{-2} , the band-gap shift is about $10^{-3}\omega_0$ [see the inset of Fig. 2(b)]. For a more realistic relative change of $\varepsilon'_H(\omega_0)$, say, of the order of 10^{-3} achievable by the optical Kerr effect, numerical computations (not shown) indicate a smaller band-gap shift of about $10^{-4}\omega_0$. Even in this case, the band-gap shift is still much larger than the modification caused by (small) material absorption, as it is seen from Fig. 5. Therefore, one can safely say that reasonably small material absorption does not significantly affect the device operation. It should be noted that the spontaneous decay rate given by (1) is the total rate, which takes into account radiative decay via both propagating and evanescent waves and, for absorbing matter, also nonradiative decay. For a detailed analysis, a better measure of the efficiency of the photon emission process may be the far-zone emission pattern and the (total) amount of radiative

energy sent out.

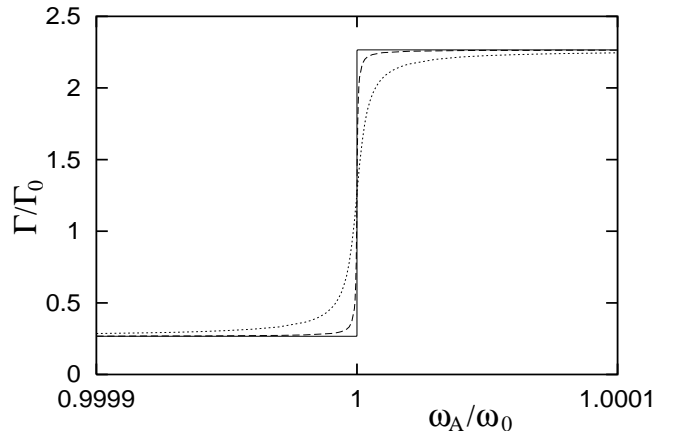


FIG. 5. The effect of material absorption on the dipole decay rate in Fig. 2(b) is shown for $\varepsilon_H(\omega)$ according to Eq. (8) with $\gamma = 10^{-7}\omega_0$ (solid line), $\gamma = 10^{-3}\omega_0$ (dashed line), and $\gamma = 10^{-2}\omega_0$ (dotted line) [$\omega_T = 20\omega_0$, $\omega_P = 1.7299\omega_T$]. The other parameters are the same as in Fig. 2(b).

Although we have given numerical examples only for symmetric configurations, the theory is applicable for arbitrary planarly stratified media. Nonsymmetric structures with a better reflecting wall on one side, which can improve the light collection efficiency on the other side of the structure, are of special interest. Another possible improvement of the device is a better photon confinement, e.g., by enclosing the emitter in micropillars or two-, or three-dimensional band-gap structures, so that a more drastic switching of the photonic density of states can be achieved. Besides the intensity-dependent Kerr nonlinearity, fast switching of photonic density of states in photonic crystals can also be achieved by using, e.g., two-photon excitation of free carriers [33].

The authors acknowledge discussions with S. Scheel. This work was supported by the Deutsche Forschungsgemeinschaft.

* On leave from the Institute of Physics, National Center for Natural Sciences and Technology, 1 Mac Dinh Chi Street, District 1, Ho Chi Minh city, Vietnam.

- [1] N. Gisin, G. Ribordy, W. Tittel, and H. Zbinden, *Rev. Mod. Phys.* **74**, 145 (2002).
- [2] E. Knill, R. Laflamme, and G. J. Milburn, *Nature (London)* **409**, 46 (2001).
- [3] X. Maître, E. Hagley, G. Nogues, C. Wunderlich, P. Goy, M. Brune, J. M. Raimond, and S. Haroche, *Phys. Rev. Lett.* **79**, 769 (1997).
- [4] B. T. H. Varcoe, S. Brattke, M. Weidinger, and H. Walther, *Nature (London)* **403**, 743 (2000).

- [5] S. Brattke, B. T. H. Varcoe, and H. Walther, Phys. Rev. Lett. **86**, 3534 (2001).
- [6] A. Kuhn, M. Hennrich, and G. Rempe, Phys. Rev. Lett. **89**, 067901 (2002).
- [7] J. Kim, O. Benson, H. Kan, and Y. Yamamoto, Nature (London) **397**, 500 (1999).
- [8] C. Kurtsiefer, S. Mayer, P. Zarda, and H. Weinfurter, Phys. Rev. Lett. **85**, 290 (2000).
- [9] R. Brouri, A. Beveratos, J.-P. Poizat, and P. Grangier, Opt. Lett. **25**, 1294 (2000).
- [10] A. Beveratos, S. Kühn, R. Brouri, T. Gacoin, J.-P. Poizat, and P. Grangier, Eur. Phys. J. D **18**, 191 (2002).
- [11] F. De Martini, G. Di Giuseppe, and M. Marrocco, Phys. Rev. Lett. **76**, 900 (1996).
- [12] S. C. Kitson, P. Jonsson, J. G. Rarity, and P. R. Tapster, Phys. Rev. A **58**, 620 (1998).
- [13] C. Brunel, B. Lounis, P. Tamarat, and M. Orrit, Phys. Rev. Lett. **83**, 2722 (1999).
- [14] B. Lounis and W. E. Moerner, Nature (London) **407**, 491 (2000).
- [15] L. Fleury, J.-M. Segura, G. Zumofen, B. Hecht, and U. P. Wild, Phys. Rev. Lett. **84**, 1148 (2000).
- [16] F. Treussart, A. Clouqueur, C. Grossman, and J.-F. Roch, Opt. Lett. **26**, 1504 (2001); F. Treussart, R. Alléaume, V. Le Floch, L. T. Xiao, J.-M. Courty, and J.-F. Roch, Phys. Rev. Lett. **89**, 093601 (2002).
- [17] P. Michler, A. Imamoglu, M. D. Mason, P. J. Carson, G. F. Strouse, and S. K. Buratto, Nature (London) **406**, 968 (2000); P. Michler, A. Kiraz, C. Becher, W. V. Schoenfeld, P. M. Petroff, L. Zhang, E. Hu, and A. Imamoglu, Science **290**, 2282 (2000).
- [18] V. Zwiller, H. Blom, P. Jonsson, N. Panev, S. Jeppesen, T. Tsegaye, E. Goobar, M.-E. Pistol, L. Samuelson, and G. Björk, Appl. Phys. Lett. **78**, 2476 (2001).
- [19] C. Santori, M. Pelton, G. Solomon, Y. Dale, and Y. Yamamoto, Phys. Rev. Lett. **86**, 1502 (2001).
- [20] E. Moreau, I. Robert, J. M. Gérard, I. Abram, L. Manin, and V. Thierry-Mieg, Appl. Phys. Lett. **79**, 2865 (2001).
- [21] Z. Yuan, B. E. Kardynal, R. M. Stevenson, A. J. Shields, C. J. Lobo, K. Cooper, N. S. Beattie, D. A. Ritchie, and M. Pepper, Science **295**, 102 (2002).
- [22] J. M. Gérard, B. Gayral, and E. Moreau, quant-ph/0207115.
- [23] M. Pelton, C. Santori, J. Vuckovic, B. Zhang, and G. S. Solomon, J. Plant, Y. Yamamoto, quant-ph/0208054.
- [24] S. Scheel, H. Häffner, H. Lee, D. V. Strekalov, P. L. Knight, and J. P. Dowling, quant-ph/0207075.
- [25] A. Kamli and M. Babiker, Phys. Rev. A **62**, 043804 (2000).
- [26] G. X. Li, F. L. Li, and S. Y. Zhu, Phys. Rev. A **64**, 013819 (2001).
- [27] N. Danz, R. Waldhäusl, A. Bräuer, and R. Kowarschik, J. Opt. Soc. Am. B **19**, 412 (2002).
- [28] K. Bergmann, H. Theuer, and B. W. Shore, Rev. Mod. Phys. **70**, 1003 (1998).
- [29] G. S. Agarwal, Phys. Rev. A **12**, 1475 (1975); J. M. Wylie and J. E. Sipe, Phys. Rev. A **30**, 1185 (1984); Ho Trung Dung, L. Knöll, and D.-G. Welsch, Phys. Rev. A **62**, 0538041 (2000).
- [30] S. Scheel, L. Knöll, and D.-G. Welsch, Phys. Rev. A **60**, 4094 (1999).
- [31] M. S. Tomáš, Phys. Rev. A **51**, 2545 (1995); W. C. Chew, *Waves and Fields in Inhomogeneous Media* (IEEE Press, New York, 1995).
- [32] M. Paulus, P. Gay-Balmaz, and O. J. F. Martin, Phys. Rev. E **62**, 5797 (2000).
- [33] P. M. Johnson, A. F. Koenderink, and W. L. Vos, Phys. Rev. B **66**, 081102(R) (2002).